Wetting of reflecting plates by an active Brownian fluid

Matthieu Mangeat[1], Shauri Chakraborty[1], Adam Wysocki[1], and Heiko Rieger[1,2]

[1]Center for Biophysics & Department for Theoretical Physics, Saarland University, Saarbrücken, Germany
[2]INM – Leibniz Institute for New Materials, Campus D2 2, Saarbrücken, Germany

Introduction

Experiments and numerical evidences reported in recent literature show that, active matter gives rise to non-equilibrium steady states in presence of boundaries and obstacles. For example, using a model of active Brownian particles [1], the phenomena of wall accumulation of active particles can be obtained with the combination of Brownian motion and self-propulsion without any explicit alignment interactions [2]. Similarly, a system of self-propelled and non-interacting particles sediment under an external gravitational field with an activity-dependent sedimentation length [3, 4, 5, 6]. Recently, a minimal active lattice gas model [7], consisting of self-propelled and hardcore particles, had been introduced in an external gravitational field [8]. By inserting a thin capillary tube into the bulk-sedimented phase of active particles, it was shown that active matter exhibits capillary action. Contrary to classical passive fluids, an active scalar fluid exhibits wall wetting and capillary action in absence of any attractive forces within the system.

Here, using interacting active Brownian particles (ABP), we study the wall-wetting mechanism of active sedimenting fluid. We consider a minimal model of active particles under gravitational field, inside a two-dimensional rectangular box. An accumulation of particles near the bottom wall is observed, as well as the wetting of vertical plates by the rise of active particles against the gravity, even without any attractive force within the system. We characterize this wall-wetting by the meniscus height, calculated from stationary density profile and depending on the inter-particle repulsion. The maximum wetting height depends super-linearly on active sedimentation length for interacting ABP, and linearly for non-interacting ABP. We also observe two large vortices concentrated close to the meniscus, due to the persistence motion of ABP against the gravity. Moreover, with non-interacting ABP, a current flow is present near the boundaries for which we propose a coarse-grained description.

Interacting active Brownian particles: the model

- N circular active Brownian particles in a $L_x \times L_y$ box with reflecting boundary conditions, subject to a gravitational force along $-\mathbf{e_y}$. The positions and self-propulsion directions $\{\mathbf{r}_i(t), \theta_i(t)\}$ obey:

$$\dot{\mathbf{r}}_i = v_s \mathbf{e}_i - v_g \mathbf{e_y} + \frac{\mathbf{F}_i}{\gamma}, \qquad \dot{\theta}_i = \sqrt{2D_r}\eta.$$

- Poly-disperse ABP with diameters uniformly distributed in $a_i \in [0.8, 1.2]$.
- The i^{th} particle experiences a force given by $\mathbf{F}_i = \sum_{j=1}^{m} \mathbf{F}_{ij}$ with

$$\mathbf{F}_{ij} = \begin{cases} k(a_i + a_j - r_{ij})\hat{\mathbf{r}}_{ij}, & \forall\, r_{ij} < a_i + a_j \\ 0, & \text{otherwise} \end{cases}.$$

- Current density is calculated with:

$$\mathbf{J}(\mathbf{r}) = \frac{1}{t_s}\sum_{t=1}^{t_s} \mathbf{e}_i(t)\delta(\mathbf{r} - \mathbf{r}_i(t))$$

- Curl of the current: $A(x, y) = \partial_x J_y - \partial_y J_x$.
- Parameters: swimming Péclet number $\mathrm{Pe}_s = v_s/aD_r$, ratio of velocities $\alpha = v_g/v_s$ and strength of repulsion between the particles $F_0 = ka/\gamma v_s$, where $a = \frac{1}{N}\sum_{i=1}^{N} a_i$.

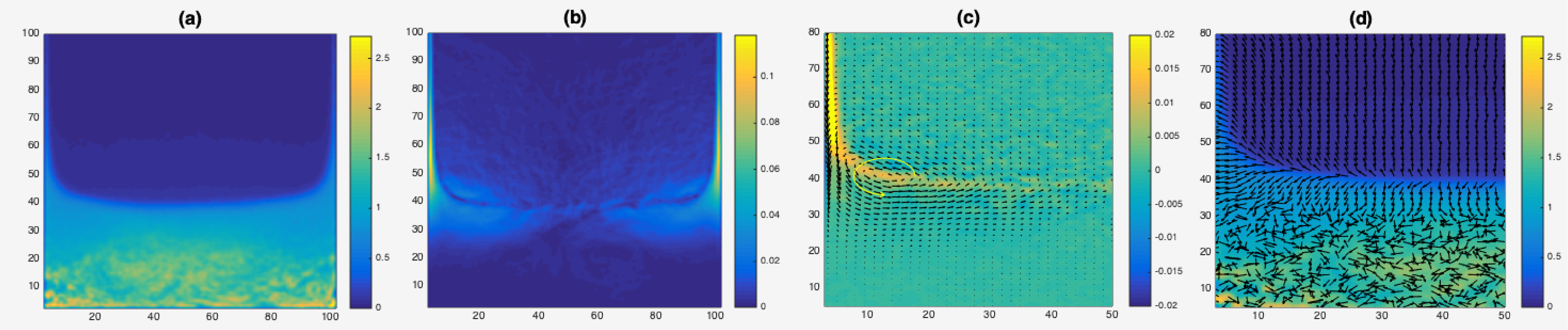

(a) Steady state density $\rho_s(x, y)$ measured for $N = 5000$ active Brownian particles under gravity in a 100×400 box. The global density is $\rho_0 = 0.125$ and the global packing fraction is $\langle\phi_0\rangle \sim 0.098$. (b) Magnitude of the current density $|\mathbf{J}_s(x, y)|$. (c) Current flow and curl amplitude $A(x, y)$ near the left boundary wall. (d) Average particle orientations $\langle\phi(x, y)\rangle$ near the left boundary wall [colormap=density].

Interacting ABP: maximum wetting height

- Far from the bottom wall, the density writes $\rho_s(x, y) \propto \exp(-y/\lambda_{\text{sed}})$ with $\lambda_{\text{sed}} \sim \mathrm{Pe}_s^2/\mathrm{Pe}_g$.
- Strong particle accumulation near the bottom wall (motility induced phase separation).

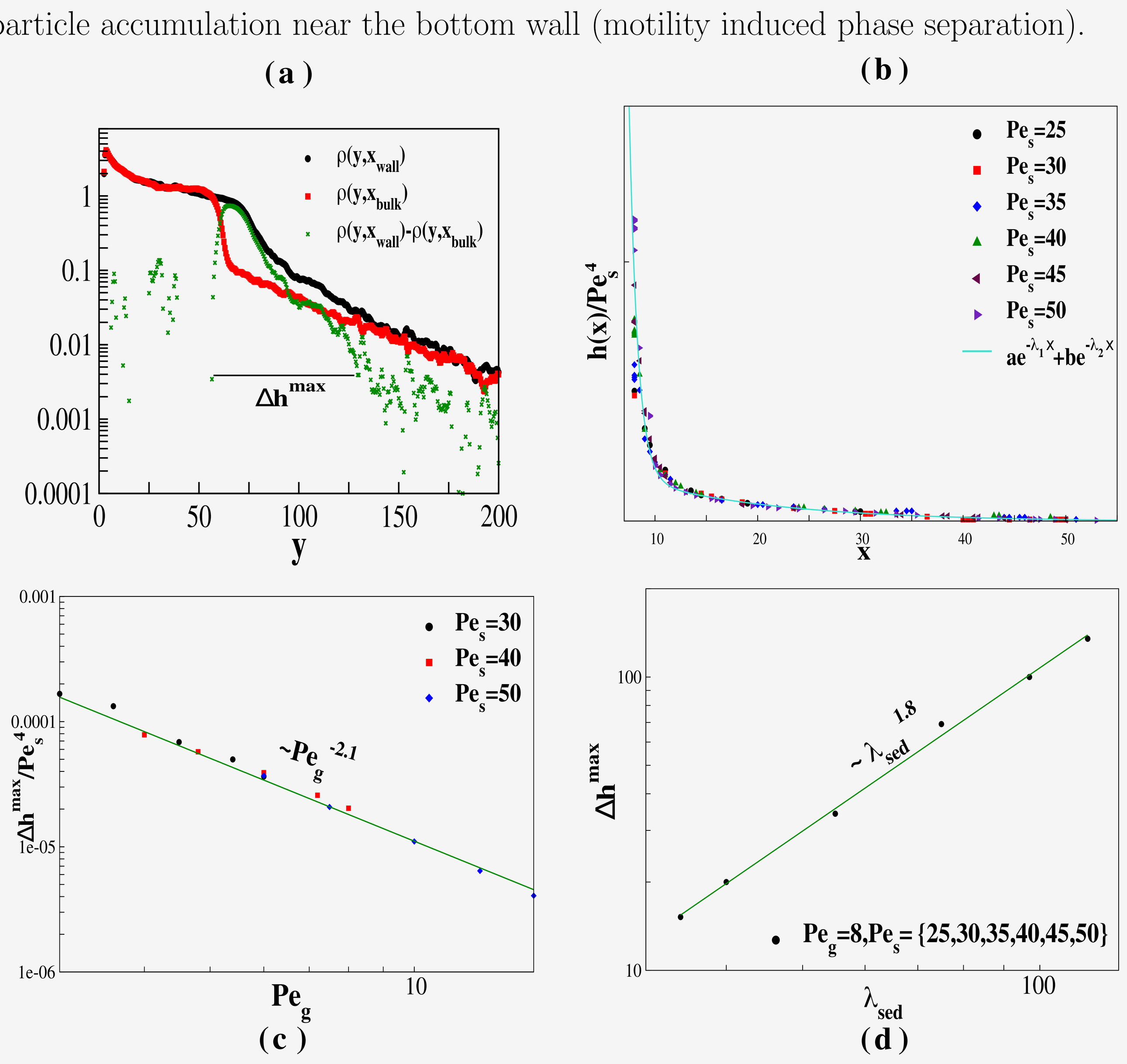

(a) Wall and bulk density profiles: $\rho(x_{\text{wall}}, y)$ and $\rho(x_{\text{bulk}}, y)$ for $\mathrm{Pe}_s = 50$, $\alpha = 0.4$, and $F_0 = 20$. The maximum wetting height $\Delta h^{\max}$ is estimated from the difference curve such that $|\rho(y, x_{\text{wall}}) - \rho(y, x_{\text{bulk}})| > 0.01$. (b) Decay of the rescaled iso-density profile $h(x)/\mathrm{Pe}_s^4$, fitted by a double-exponential function. (c) Maximum wetting height $\Delta h^{\max} \sim \mathrm{Pe}_s^4/\mathrm{Pe}_g^{2.1}$. (d) Maximum wetting height $\Delta h^{\max} \sim \lambda_{\text{sed}}^{1.8}$.

- Maximum wetting height behaves like $\Delta h \sim \lambda_{\text{sed}}^2$.

Interacting ABP: vortices

- Characterization of the large vortices near the wetting layer on the left and right plates.
- Total bulk enstrophy is defined by

$$\varepsilon = \int_{\rho > \rho_{\text{iso}}} dx dy\, |A(x, y)|^2.$$

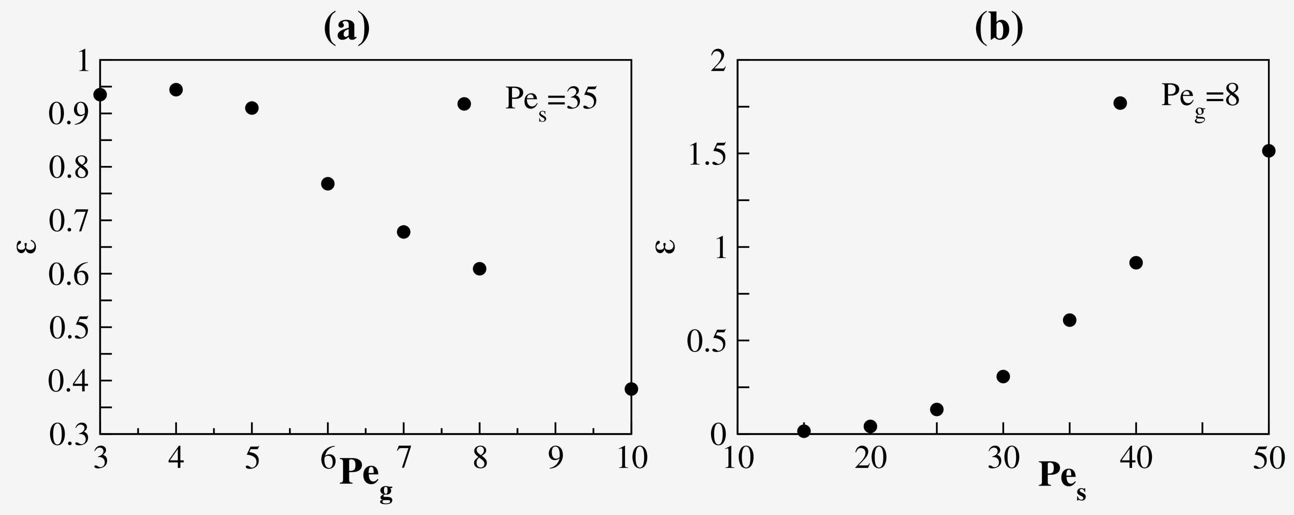

(a) Enstrophy decreases with Pe_g for a fixed $\mathrm{Pe}_s = 35$. (b) Enstrophy increases with Pe_s for fixed $\mathrm{Pe}_g = 8$.

Non-interacting active Brownian particles ($F_0 = 0$)

- Pointlike active Brownian particles in a $L_x \times L_y$ box with reflecting boundary conditions under gravitational force. The position and self-propulsion direction $\{\mathbf{r}(t), \theta(t)\}$ obey:

$$\dot{\mathbf{r}} = v_s \mathbf{e}_\theta - v_g \mathbf{e_y} + \sqrt{2D_t}\boldsymbol{\eta}_r, \qquad \dot{\theta} = \sqrt{2D_r}\eta_\theta.$$

- Corresponding Fokker-Planck equation for the probability density function $p(\mathbf{r}, \theta; t)$:

$$\partial_t p = \nabla \cdot [D_t \nabla p - (v_p \mathbf{e}_\theta - v_g \mathbf{e_y})p] + D_r \partial_\theta^2 p.$$

- With density $\rho(\mathbf{r}) = \int d\theta p(\mathbf{r}, \theta)$ and magnetization $\mathbf{m}(\mathbf{r}) = \int d\theta \mathbf{e}_\theta p(\mathbf{r}, \theta)$, the current density writes

$$\mathbf{J} = -D_t \nabla \rho - v_p \mathbf{m} + v_g \rho \mathbf{e_y}.$$

- Curl of the current: $A(x, y) = \partial_x J_y - \partial_y J_x = -v_p[\partial_x m_y - \partial_y m_x] + v_g \partial_x \rho$.
- Parameters: swimming Péclet number $\mathrm{Pe}_s = v_s/\sqrt{D_t D_r}$, and ratio of velocities $\alpha = v_g/v_s = \mathrm{Pe}_g/\mathrm{Pe}_s$.

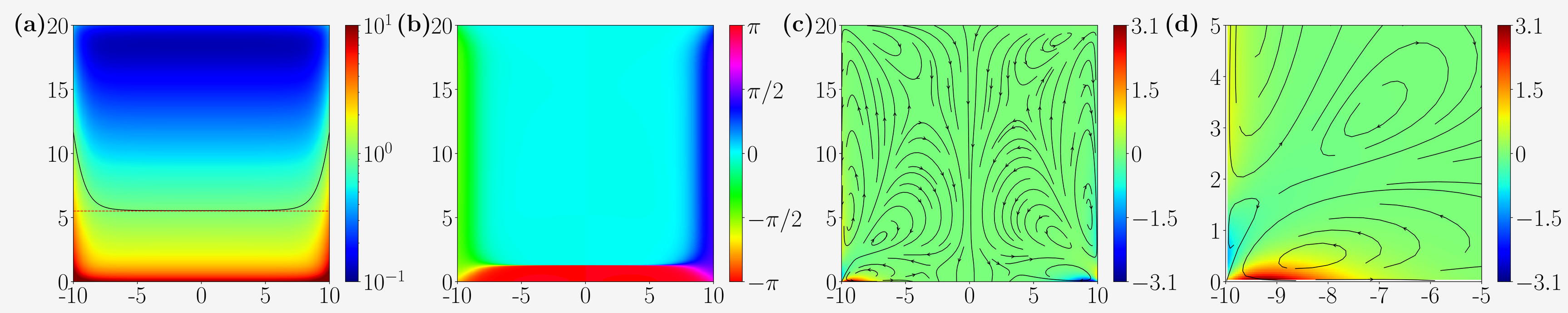

(a) Steady state density ρ_s. (b) Mean orientation given by the magnetization $\mathbf{m}_s$. (c) Current flow given by the orientation of $\mathbf{J}_s$ and curl amplitude $A(x, y)$. (d) Zoom on the bottom-left corner of (c). Parameters: $\mathrm{Pe}_s = 2$ and $\alpha = 0.25$.

Non-interacting ABP: maximum wetting height

- Far from top and bottom walls, the density writes $\rho_s(x, y) = f(x)\exp(-y/\lambda_{\text{sed}})$ with $\lambda_{\text{sed}} = \mathrm{Pe}_s^2/\mathrm{Pe}_g$.

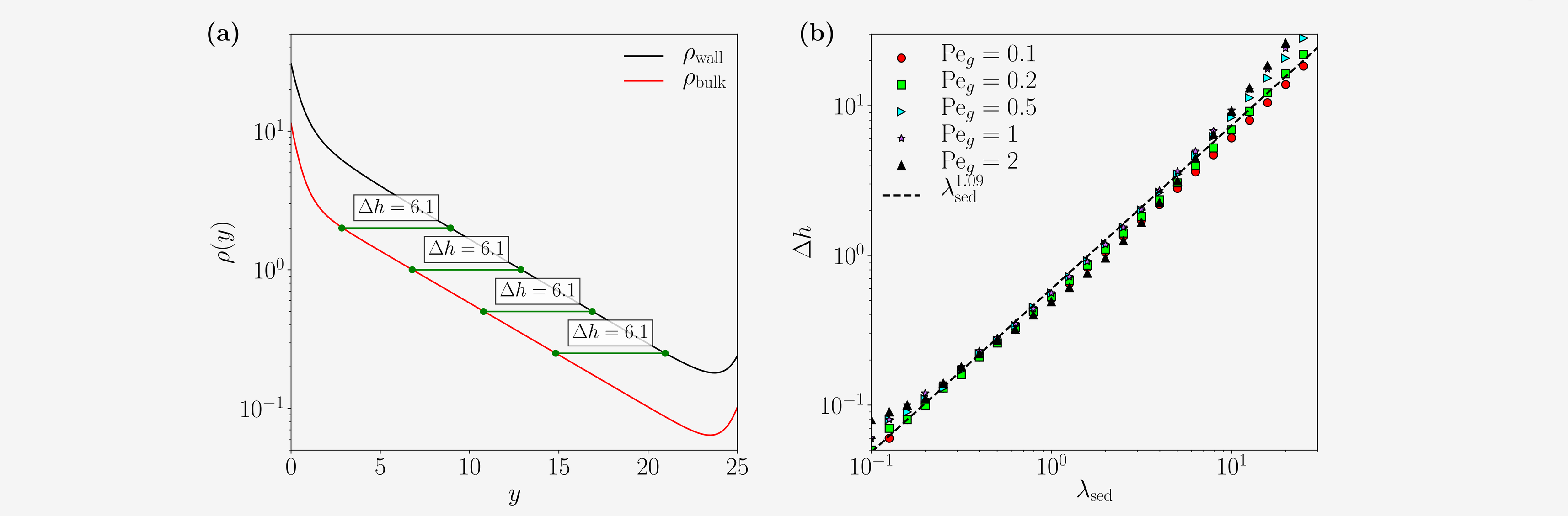

(a) Wall and bulk density profiles: $\rho_{\text{wall}} = \rho(x_{\text{wall}}, y)$ and $\rho_{\text{bulk}} = \rho(x_{\text{wall}}, y)$ for $\mathrm{Pe}_s = 2$ and $\alpha = 0.25$. In the exponential decay regime, $\Delta h = 6.1$. (b) Maximum wetting height Δh as a function of $\lambda_{\text{sed}} = \mathrm{Pe}_s^2/\mathrm{Pe}_g$.

- Maximum wetting height behaves like $\Delta h \sim \lambda_{\text{sed}}$.

Non-interacting ABP: vortices

- Vortices formed by the current flows are localized in the four corners, and deformed by the gravity field.

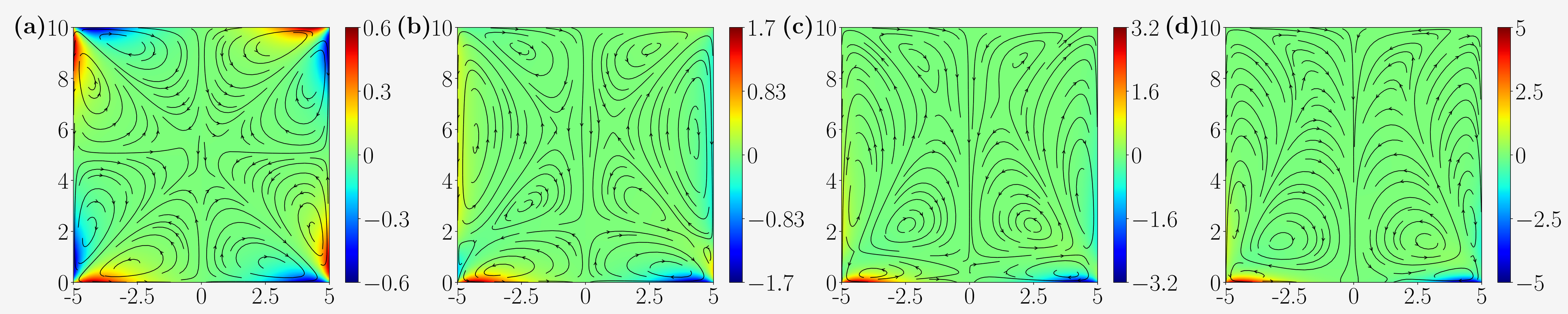

Current flow given by the orientation of $\mathbf{J}_s$ and curl amplitude $A(x, y)$. Parameters: $\mathrm{Pe}_s = 2$ and (a) $\alpha = 0$, (b) $\alpha = 0.25$, (c) $\alpha = 0.5$, and (d) $\alpha = 0.75$.

- Vortex area decreases with Pe_s and α, while the maximum curl amplitude increases.

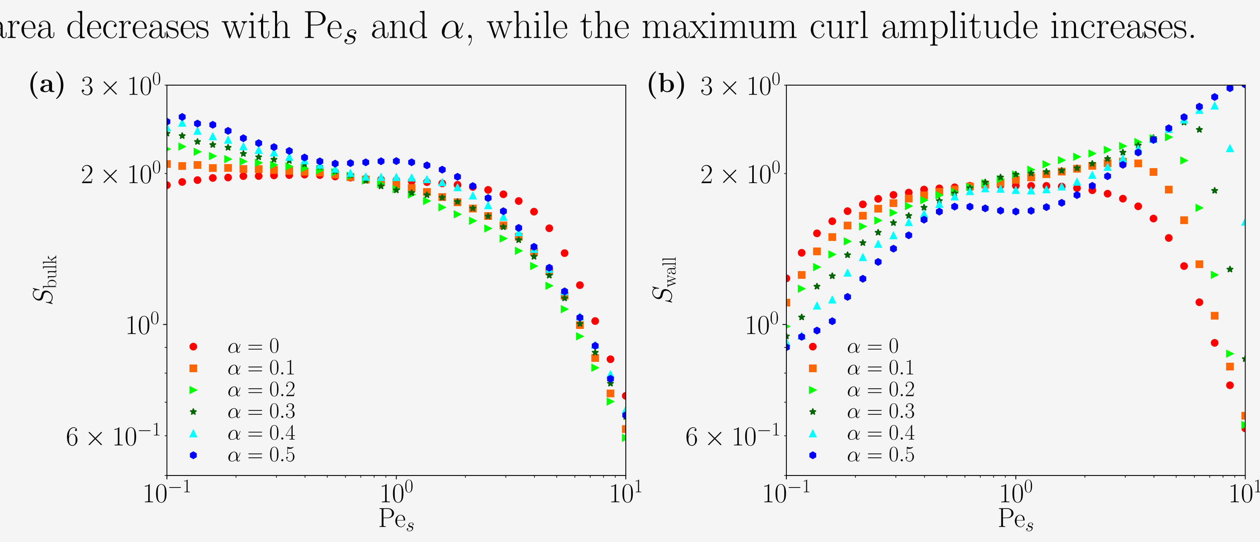

Vortex area S_{bulk} (a) and S_{wall} (b) located close to the bottom and left walls, respectively.

References

[1] A. P. Solon, M. E. Cates, and J. Tailleur, Eur. Phys. J. Spec. Top. **224**, 1231-1262 (2015).
[2] J. Elgeti and G. Gompper, EPL **101**, 48003 (2003).
[3] J. Palacci, C. Cottin-Bizonne, C. Ybert, and L. Bocquet, Phys. Rev. Lett. **105**, 088304 (2010).
[4] F. Ginot, I. Theurkauff, D. Levis, C. Ybert, L. Bocquet, L. Berthier, and C. Cottin-Bizonne, Phys. Rev. X **5**, 011004 (2015).
[5] F. Ginot, A. Solon, Y. Kafri, C. Ybert, J. Tailleur, and C. Cottin-Bizonne, New J. Phys. **20**, 115001 (2018).
[6] S. Hermann and M. Schmidt, Soft Matter **14**, 1614-1621 (2018).
[7] M. Kourbane-Houssene, C. Erignoux, T. Bodineau, and J. Tailleur, Phys. Rev. Lett. **120**, 268003 (2018).
[8] A. Wysocki and H. Rieger, Phys. Rev. Lett. **124**, 048001 (2020).

Acknowledgements

This work was financially supported by the German Research Fondation (DFG) within the Collaborative Research Center SFB 1027.

mangeat@lusi.uni-sb.de